Inorg. Chem. **2007**, *46*, 1250–1258

A New Series of Three-Dimensional Metal–Organic Framework, $[M_2(H_2O)][C_5N_1H_3(COO)_2]_3 \cdot 2H_2O$, M = La, Pr, and Nd: Synthesis, Structure, and Properties

Partha Mahata and Srinivasan Natarajan*

Framework Solids Laboratory, Solid State and Structural Chemistry Unit, Indian Institute of Science, Bangalore 560 012, India

Received September 18, 2006

A new series of lanthanide pyridine dicarboxylates of the general formula, $[M_2(H_2O)][C_5N_1H_3(COO)_2]_3 \cdot 2H_2O$, M = La (**1**), Pr (**2**), and Nd (**3**), has been prepared by the reaction of trivalent lanthanide salts and pyridine dicarboxylic acids employing a mild condition hydrothermal reaction. The structures are built up from MO_8N and MO_7N_2 (M = lanthanide) polyhedra connected to the dicarboxylate anions forming the three-dimensional structure with one-dimensional channels. A striking feature of this structure is the presence of an unusual Z-shaped tetramer of the formula $M_4O_{24}N_6$. Extraframework water molecules, located within the open channels, are reversibly adsorbed. Detailed in situ and ex situ investigations using FTIR and PXRD studies clearly show that the removal of the water molecules is reversible and accompanied by changes in the size of the channel. Partial substitution at the La sites by Eu gives rise to characteristic red-pink luminescence, indicating a ligand-sensitized metal-centered emission.

Introduction

Metal−organic frameworks (MOFs) with open structures are widely regarded as promising materials for many applications, such as catalysis, separation, gas storage, sensing, magnetism, and ion exchange.[1−6] Compared with the conventional microporous inorganic materials such as zeolites, the MOFs appear to be more flexible for rational design, through control of the architecture and functionalization of the pores. Much work has been carried out employing multifunctional ligands for the preparation of transition-metal carboxylates.[7−9] In contrast, the design and synthesis of lanthanide-based MOFs appears to be a formidable task primarily due to the varied coordination requirements of the lanthanide ions.[10,11] However, lanthanides, with their high and variable coordination numbers and flexible coordination environment, provide unique opportunities for the discovery of unusual network topologies.[12,13] We have been interested in the study of benzene dicarboxylate-based coordination polymers of lanthanides and related systems, which has resulted in the formation of many interesting structures.[14−16] In continuation of the theme, we are now studying the reactions involving pyridine dicarboxylic acids. The use of pyridine-2,3-dicarboxylic acid as the ligand in the formation of MOF compounds has been limited,[17−19]

* To whom correspondence should be addressed. E-mail: snatarajan@sscu.iisc.ernet.in.

(1) Ferey, G.; Draznieks, C. M.; Serre, C.; Millange, F.; Dutour, J.; Surble, S.; Margiolaki, I. *Science* **2005**, *309*, 2040.
(2) Lin, X.; Blake, A. J.; Wilson, C.; Sun, X. M.; Champness, N. R.; George, M. W.; Hubberstey, P.; Mokaya, R.; Schröder, M. *J. Am. Chem. Soc.* **2006**, *128*, 10745.
(3) Chandler, B. D.; Cramb, D. T.; Shimizu, G. K. H. *J. Am. Chem. Soc.* **2006**, *128*, 10403.
(4) Wong-Foy, A. G.; Matzger, A. J.; Yaghi, O. M. *J. Am. Chem. Soc.* **2006**, *128*, 3494.
(5) Rao, C. N. R.; Natarajan, S.; Vaidhyanathan, R. *Angew. Chem., Int. Ed.* **2004**, *43*, 1466.
(6) Bu, X. H.; Tong, M. L.; Chang, H. C.; Kitagawa, S.; Batten, S. R. *Angew. Chem., Int. Ed.* **2004**, *43*, 192.
(7) Zhang, J. P.; Lin, Y. Y.; Huang, X. C.; Chen, X. M. *J. Am. Chem. Soc.* **2005**, *127*, 5495.
(8) Zheng, J. M.; Batten, S. R.; Du, M. *Inorg. Chem.* **2005**, *44*, 3317.
(9) Nakabayashi, K.; Kawaano, M.; Yoshizawa, M.; Ohkoshi, S. I.; Fujita, M. *J. Am. Chem. Soc.* **2004**, *126*, 16694.
(10) Guo, X. D.; Zhu, G. S.; Fang, Q. R.; Xue, M.; Tian, G.; Sun, J. Y.; Li, X. T.; Qui, S. L. *Inorg. Chem.* **2005**, *44*, 3850.
(11) Zhao, B.; Cheng, P.; Chen, X. Y.; Cheng, C.; Shi, W.; Liao, D. Z.; Yan, S. P.; Jiang, Z. H. *J. Am. Chem. Soc.* **2004**, *126*, 3012.
(12) Zhang, M. B.; Zhang, J.; Zheng, S. T.; Yang, G. Y. *Angew. Chem., Int. Ed.* **2005**, *44*, 1385.
(13) Devic, T.; Serre, C.; Audebrand, N.; Marrat, J.; Ferey, G. *J. Am. Chem. Soc.* **2005**, *127*, 12788.
(14) Thirumurugan, A.; Natarajan, S. *J. Mater. Chem.* **2005**, *15*, 4588.
(15) Thirumurugan, A.; Natarjan, S. *Dalton Trans.* **2004**, 2923.
(16) Thirumurugan, A.; Natarajan, S. *Cryst. Growth Des.* **2006**, *6*, 983.
(17) Yu, Z. T.; Liao, Z. L.; Jiang, Y. S. Li, G. H.; Li, G. D.; Chen, J. S. *Chem. Commun.* **2004**, 1814.
(18) Mahata, P.; Sankar, G.; Madras, G.; Natarajan, S. *Chem. Commun.* **2005**, 5787.

10.1021/ic0617644 CCC: $37.00
Published on Web 01/13/2007

compared with other pyridine dicarboxylic acids.[20−28] This is probably due to the following reasons: (i) It often behaves like picolinic acid, acting as a chelating bidentate ligand through the nitrogen atom and one oxygen atom of the carboxylic acid group in ortho position, and the second carboxylic acid group remains idle.[29−31] (ii) It prefers decarboxylation of the carboxylic acid group in the ortho position and transforms to nicotinic acid.[32−33] During the course of our study, we have now prepared a new series of lanthanide MOF compounds of the general formula, $[M_2(H_2O)][C_5N_1H_3(COO)_2]_3{\cdot}2H_2O$, M = La (**1**), Pr (**2**), and Nd (**3**). The structures of the compounds are identical and are formed by MO_8N and MO_7N_2 polyhedral units connected by dicarboxylate anions giving rise to the three-dimensional structure. The extraframework water molecules can be reversibly absorbed. Doping of 2 and 4% Eu^{3+}, in place of La^{3+}, clearly show metal-centered emission. In this paper, we present the synthesis, structure, guest exchange, and luminescent properties.

Experimental Section

Synthesis and Initial Characterization. The reactants needed for the synthesis of the title compounds, $La(NO_3)_3$, $Pr(NO_3)_3$, $Nd(NO_3)_3$, $Eu(NO_3)_3$ (99.9%, Terio Corporation, Qingdao, China), and pyridine-2,3-dicarboxylic acid (99%, Lancaster), were used as purchased. The water used was double-distilled through a Millipore membrane. All the compounds were prepared by hydrothermal methods. In a typical synthesis, for **1**, $La(NO_3)_3$ (0.325 g, 1 mM) was dissolved in 14 mL of water. Pyridine-2,3-dicarboxylic (0.338 g, 2 mM) was then added, with continuous stirring, and the mixture was homogenized at room temperature for 30 min. The final mixture was then sealed in a 23 mL PTFE-lined stainless steel acid digestion autoclave and heated at 140 °C for 72 h. The initial pH value of the reaction mixture was 3, and no appreciable change in pH was noted after the reaction. The final product, containing large quantities of colorless rectangular crystal, was filtered, washed with deionized water under vacuum, and dried at ambient conditions (yield 70% based on La). For **2** and **3**, $Pr(NO_3)_3$ (0.327 g, 1 mM) and $Nd(NO_3)_3$ (0.3308 g, 1 mM) were used in place of $La(NO_3)_3$ by keeping composition and procedures identical to those in **1**. In both cases, the resulting product contained large quantities of pale-green (**2**) and pale-violet (**3**) crystals with similar yields. For the preparation of Eu-doped compounds (2 mol %, **1a**, and 4 mol %, **1b**), we also employed a similar synthesis procedure resulting in a fine uniform powder. Anal. Calcd for **1**: C 30.47, H 1.81, N 5.08. Found: C 30.2, H 1.88, N 5.11. Anal. Calcd for **2**: C 30.32, H 1.80, N 5.05. Found: C 30.5, H 1.77, N 5.09. Anal. Calcd for **3**: C 30.07, H 1.79, N 5.01. Found: C 30.15, H 1.84, N 5.08. Anal. Calcd for **1a**: C 30.46, H 1.81, N 5.08. Found: C 30.40, H 1.77, N 5.12. Anal. Calcd for **1b**: C 30.44, H 1.81, N 5.07. Found: C 30.51, H 1.75, N 5.13.

Table 1. The Observed IR Bands for $[La_2(H_2O)][C_5N_1H_3(COO)_2]_3{\cdot}2H_2O$ (**1**), $[Pr_2(H_2O)][C_5N_1H_3(COO)_2]_3{\cdot}2H_2O$ (**2**), and $[Nd_2(H_2O)][C_5N_1H_3(COO)_2]_3{\cdot}2H_2O$ (**3**)

bands	**1** (cm^{-1})	**2** (cm^{-1})	**3** (cm^{-1})
ν_{as}(O−H)	3488 (s)	3495 (s)	3497 (s)
ν_s(C−H)$_{aromatic}$	3067 (w)	3060 (w)	3064 (w)
ν_s(C═O)	1612 (s)	1620 (s)	1617 (s)
$\delta(H_2O)$	1574 (s)	1577 (s)	1582 (s)
ν_s(C−C)$_{skeletal}$	1544 (m)	1551 (m)	1550 (m)
δ(COO)	1372 (s)	1367 (s)	1368 (s)
δ(CH$_{aromatic}$)$_{in-plane}$	1267 (w)	1266 (w)	1269 (w)
δ(C−N)$_{skeletal}$	835 (s)	840 (s)	832 (s)
δ(CH$_{aromatic}$)$_{out-of-plane}$	780 (m)	776 (m)	782 (m)

Powder X-ray diffraction (XRD) patterns were recorded on crushed single crystals in the 2θ range of 5−50° using Cu Kα radiation (Philips X'Pert). The XRD patterns indicated that the products were new materials, the patterns being entirely consistent with the simulated XRD pattern generated based on the structures determined using the single-crystal XRD. IR spectra were recorded on KBr plates (Perkin-Elmer, SPECTRUM 1000). The observed IR frequencies are listed in Table 1. The mid-IR range studies did not reveal bands corresponding to metal−ligand modes, as they appear lower than the 400 cm^{-1} range. The thermogravimetric analyses were carried out (Metler-Toledo) in an oxygen atmosphere (flow rate = 50 mL/min) in the temperature range of 30−850 °C (heating rate = 5 °C/min). The results indicate all three compounds behave in a similar fashion. An initial weight loss (~6.5%) in the temperature range of 200−250 °C for all three compounds may be due to the loss of the extraframework and coordinated water molecules, and the second sharp weight loss in the temperature range of 380−430 °C corresponds with the loss of the carboxylate. The total observed weight loss corresponds well with the loss of the carboxylate and the water molecules 58% (calc 60%), 61% (calc 59%), and 55% (calc 59.8%), respectively, for **1**, **2**, and **3**. The final calcined product was found to be crystalline by powder XRD and corresponds to La_2O_3 (JCPDS No. 00-002-0688), Pr_6O_{11} (JCPDS No. 00-042-1121), and Nd_2O_3 (JCPDS Nos. 00-021-0579 and 00-006-0408), respectively.

Single-Crystal Structure Determination. A suitable single crystal of each compound was carefully selected under a polarizing microscope and carefully glued to a thin glass fiber. The single-crystal data were collected on a Bruker AXS smart Apex CCD diffractometer at 293(2) K. The X-ray generator was operated at 50 kV and 35 mA using Mo Kα (λ = 0.71073 Å) radiation. Data were collected with a ω scan width of 0.3°. A total of 606 frames were collected in three different settings of φ (0, 90, 180°), keeping the sample-to-detector distance fixed at 6.03 cm and the detector position (2θ) fixed at −25°. The data were reduced using SAINT-PLUS,[34] and an empirical absorption correction was applied using the SADABS program.[35] The structure was solved and refined using

(19) Yue, Q.; Yang, J.; Li, G. H.; Li, G. D.; Xu, W.; Chen, J. S.; Wang, S. N. *Inorg. Chem.* **2005**, *44*, 5241.
(20) Garcia-Zarracino, R.; Höpfl, H. *Angew. Chem., Int. Ed.* **2004**, *43*, 1507.
(21) Humphery, S. M.; Wood, P. T. *J. Am. Chem. Soc.* **2004**, *126*, 13236.
(22) Liu, Y. L.; Kravtsov, V. C.; Beauchamp, D. A.; Eubank, J. F.; Eddaoudi, M. *J. Am. Chem. Soc.* **2005**, *127*, 7266.
(23) Wei, Y. L.; Hou, H. W.; Li, L. K.; Fan, Y. T.; Zhou, Y. *Cryst. Growth Des.* **2005**, *5*, 1405.
(24) Zhao, B.; Cheng, P.; Dai, Y.; Cheng, C.; Liao, D. Z.; Yan, S. P.; Jiang, Z. H.; Wang, G. L. *Angew. Chem., Int. Ed.* **2003**, *42*, 934.
(25) Zhao, B.; Gao, H. L.; Chen, X. Y.; Cheng, P.; Shi, W.; Liao, D. Z.; Yan, S. P.; Jiang, Z. H. *Chem.—Eur. J.* **2006**, *12*, 149.
(26) Gao, H. L.; Yi, Long.; Zhao, B.; Zhao, X. Q.; Cheng, P.; Laio, D. Z.; Yan, S. P. *Inorg. Chem.* **2006**, *45*, 5980.
(27) Ghosh, S. K.; Bharadwaj, P. K. *Inorg. Chem.* **2003**, *42*, 8250.
(28) Ghosh, S. K.; Bharadwaj, P. K. *Inorg. Chem.* **2005**, *44*, 3156.
(29) Suga, T.; Okabe, N. *Acta Crystallogr.* **1996**, *C52*, 1410.
(30) Okabe, N.; Miura, J.; Shimosaki, A. *Acta Crystallogr.* **1996**, *C52*, 1610.
(31) Sengupta, P.; Ghosh, S.; Mark, T. C. W. *Polyhedron* **2001**, *20*, 975.
(32) Chen, W.; Yuan, H. M.; Wang, J. Y.; Liu, Z. Y.; Xu, J. J.; Yang, M.; Chen, J. S. *J. Am. Chem. Soc.* **2003**, *125*, 9266.
(33) Gerrard, L. A.; Wood, P. T. *Chem. Commun.* **2000**, 2107.
(34) *SMART* (V 5.628), *SAINT* (V 6.45a), *XPREP*, *SHELXTL*; Bruker AXS, Inc.: Madison, WI, 2004.
(35) Sheldrick, G. M. *SADABS*; University of Göttingen: Göttingen, Germany, 1994.

Table 2. Crystal Data and Structure Refinement Parameters for $\{[M_2(H_2O)][C_5N_1H_3(COO)_2]_3 \cdot 2H_2O\}$, M = La (**1**), Pr (**2**), and Nd (**3**)

structure parameter	M = La (**1**)	M = Pr (**2**)	M = Nd (**3**)
empirical formula	$C_{21}H_{15}N_3O_{15}La_2$	$C_{21}H_{15}N_3O_{15}Pr_2$	$C_{21}H_{15}N_3O_{15}Nd_2$
fw	827.13	831.13	837.79
cryst syst	monoclinic	monoclinic	monoclinic
space group	$P2_1/c$ (No. 14)	$P2_1/c$ (No. 14)	$P2_1/c$ (No. 14)
a (Å)	9.0495(17)	8.9814(18)	8.9586(19)
b (Å)	17.355(3)	17.278(4)	17.246(4)
c (Å)	15.570(3)	15.462(10)	15.406(3)
α (deg)	90.0	90.0	90.0
β (deg)	102.570(3)	102.233(4)	102.033(4)
γ (deg)	90.0	90.0	90.0
V (Å^3)	2386.7(8)	2345.0(8)	2327.9(9)
Z	4	4	4
T (K)	293(2)	293(2)	293(2)
ρ_{calc} (g cm^{-3})	2.285	2.337	2.373
μ (mm^{-1})	3.619	4.195	4.501
θ range (deg)	1.78 to 27.98	1.79 to 28.00	1.79 to 27.99
λ (Mo Kα) (Å)	0.71073	0.71073	0.71073
R1 indices ($I > 2s(I)$)	R1 = 0.0591, wR2 = 0.1240	R1 = 0.0593, wR2 = 0.1004	R1 = 0.0770, wR2 = 0.1225
R[a] indices (all data)	R1 = 0.0978, wR2 = 0.1400	R1 = 0.0946, wR2 = 0.1111	R1 = 0.1119, wR2 = 0.1328

[a] $R1 = \Sigma||F_o| - |F_c||/\Sigma|F_o|$; $wR2 = \{\Sigma[w(F_o^2 - F_c^2)^2]/\Sigma[w(F_o^2)^2]\}^{1/2}$. $w = 1/[\sigma^2(F_o)^2 + (aP)^2 + bP]$, $P = [\max(F_o^2,0) + 2(F_c)^2]/3$, where $a = 0.0255$ and $b = 20.9261$ for **1**, $a = 0.0376$ and $b = 2.2469$ for **2**, and $a = 0.0329$ and $b = 12.0406$ for **3**.

SHELXL97[36] present in the WinGx suit of programs (Version 1.63.04a).[37] All the hydrogen atoms of the carboxylic acids were initially located in the difference Fourier maps, and for the final refinement, the hydrogen atoms were placed in geometrically ideal positions and held in the riding mode. The hydrogen atoms of the water molecule were not located in the difference Fourier maps. Final refinement included atomic positions for all the atoms, anisotropic thermal parameters for all the non-hydrogen atoms, and isotropic thermal parameters for all the hydrogen atoms. Full-matrix least-squares refinement against $|F^2|$ was carried out using the WinGx package of programs.[37] Details of the structure solution and final refinements for **1**, **2**, and **3** are given in Table 2. CCDC Nos. 620336−620338 for compounds **1**−**3** contain the crystallographic data for this paper. These data can be obtained free of charge from The Cambridge Crystallographic Data Center (CCDC) via www.ccdc.cam.ac.uk/data_request/cif.

Results and Discussion

Structure. All three compounds are isostructural and have 41 non-hydrogen atoms in the asymmetric unit. There are two crystallography independent M^{3+} ions (M = La, Pr, Nd) and three Py-2,3-dicarboxylate anions. The M^{3+} ions are connected to three Py-2,3-dicarboxylate anions and a water molecule. The three Py-2,3-dicarboxylates can be classified into three different types (acid-1, acid-2, and acid-3) on the basis of their coordination modes with the metal atoms (Figure 1a). The metal atom, M(1), is surrounded by eight oxygen atoms and one nitrogen atom and has a distorted tricapped trigonal prismatic environment ($M(1)O_8N$, CN = 9). Of these, one oxygen atom, O(3), is a coordinated water molecule, the nitrogen atom belongs to the pyridine ring, and the remaining oxygens are from the carboxylate group. Three oxygen atoms, O(2), O(6), and O(7), have μ_3 connectivity linking two metal centers and a carbon atom, whereas O(2) connects two M(1) and a carbon atom and O(6) and O(7) link M(1) and M(2) and a carbon atom. The metal atom, M(2), is coordinated by seven oxygen atoms and two nitrogen atoms forming a distorted tricapped trigonal prismatic environment ($M(2)O_7N_2$, CN = 9). The two nitrogen atoms (N(2) and N(3)) are from the pyridine rings, and the seven oxygen atoms are from the carboxylate group. The M−O bonds have distances in the range of 2.417(7)−2.774(7) Å, the M−N bonds have distances in the range of 2.602(8)−2.726(8) Å, and the O−M−O bond angles are in the range of 48.4(19)−154.95(19) Å for **1**, **2**, and **3**. The coordination environments of the central metal ions were based on an assumption of typical M−O distances in the range of 2.4−2.8 Å. The selected bond distances for the three compounds are listed in Table 3.

The three-dimensional structure of the compounds can be explained by considering smaller building units. Thus, the M(1) polyhedral units are connected through a common edge with another M(1) via a μ_3 coordinated oxygen (O(2)) forming a dimer. The dimers are, again, connected to M(2) polyhedra through two oxygen atoms, O(6) and O(7), forming a tetrameric unit of the formula, $M_4O_{24}N_6$, as shown in Figure 1b. As can be observed, the tetramer has a "Z"-like shape and the connectivity is as follows: M(2)−M(1)−M(1)−M(2). To our knowledge, this is the first observation of this type of a tetramer in MOF compounds involving lanthanides. The tetramers are connected through the acid-2 to form a two-dimensional layer (Figure 2a). The layers, in turn, are connected by acid-1 and acid-3 to give rise to the three-dimensional structure with one-dimensional channels. The extraframework water molecules occupy the channels. Of the two water molecules, O(200) appears to have weak hydrogen bond interactions with the terminal water molecule, O(3), bound with the Ln^{3+} ions (H···A = 1.92(1) Å and D−H···A = 147.1(1)°). In the *ab* plane the connectivity between the two layers is shown (Figure 2b). The connectivity between the layers through acid-1 and acid-3 resembles a molecular zipper (Figure 2b). As can be noted, the M−O polyhedra appear to have a helical arrangement, probably due to the presence of the 2-fold screw axis.

(36) Sheldrick, G. M. *SHELXL-97 Program for Crystal Structure Solution and Refinement*; University of Göttingen: Göttingen, Germany, 1997.
(37) Farrugia, J. L. WinGx Suite for Small-Molecule Single Crystal Crystallography. *J. Appl. Crystallogr.* **1999**, *32*, 837.

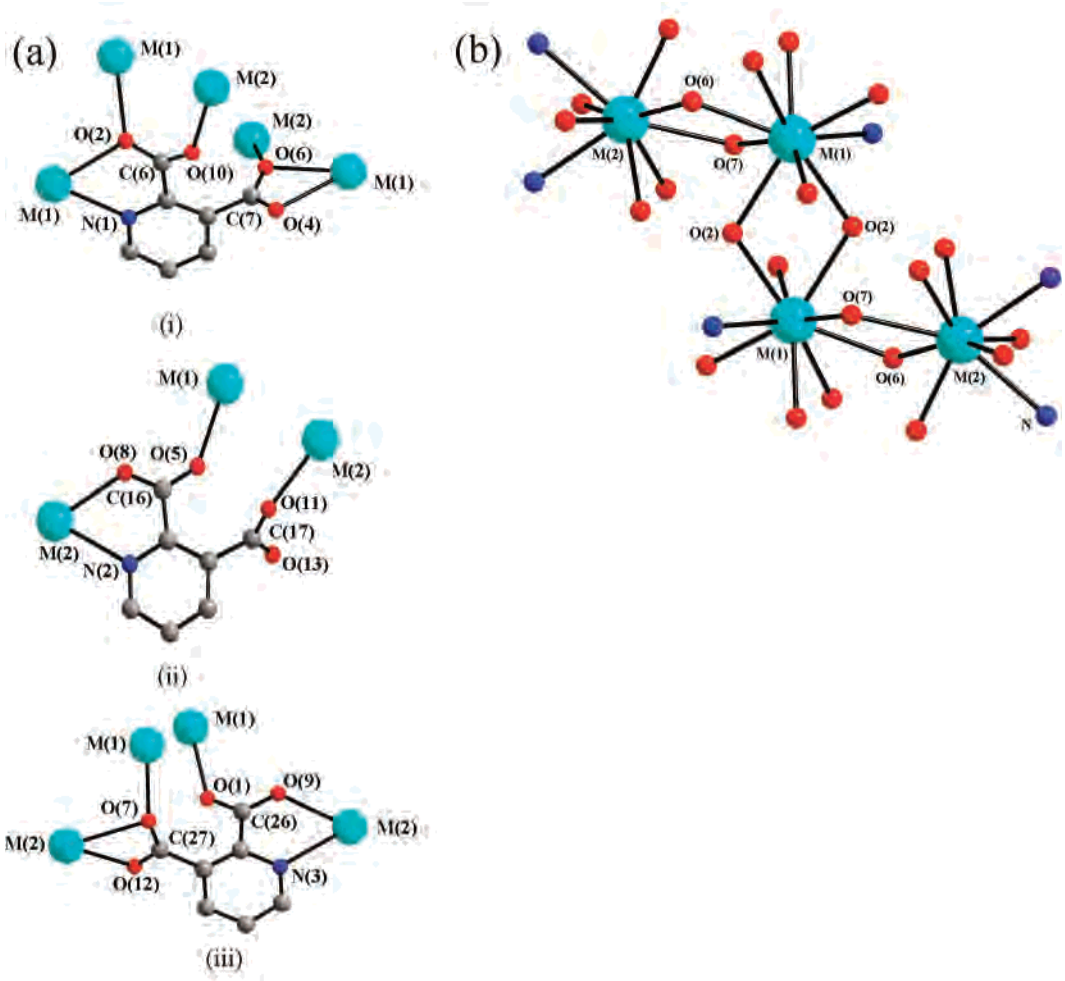

Figure 1. (a) The various coordination modes of the pyridine-2,3-dicarboxylate anions observed in $[M_2(H_2O)][C_5N_1H_3(COO)_2]_3{\cdot}2H_2O$, M = La (**1**), Pr (**2**), and Nd (**3**) ((i) acid-1, (ii) acid-2, and (iii) acid-3). (b) Connectivity between $M(1)O_8N$ and $M(2)_7N_2$ polyhedra through the μ_3 oxygen atoms. Note the formation of the "Z"-shaped $M_4O_{24}N_6$ tetrameric cluster (see text).

Table 3. Selected Bond Distances (Å) Observed in $\{[M_2(H_2O)][C_5N_1H_3(COO)_2]_3{\cdot}2H_2O\}$, M = La (**1**), Pr (**2**), and Nd (**3**)[a]

bond	M = La (**1**)	M = Pr (**2**)	M = Nd (**3**)
M(1)−O(1)	2.471(6)	2.425(6)	2.417(7)
M(1)−O(2)	2.569(6)	2.527(6)	2.512(7)
M(1)−O(3)	2.512(7)	2.493(6)	2.460(9)
M(1)−O(4)	2.774(7)	2.771(6)	2.742(8)
M(1)−O(5)	2.477(6)	2.441(5)	2.425(7)
M(1)−O(6)	2.562(6)	2.510(6)	2.489(7)
M(1)−O(7)	2.495(6)	2.463(6)	2.439(8)
M(1)−O(2)#1	2.602(6)	2.601(6)	2.593(7)
M(1)−N(1)	2.726(8)	2.686(6)	2.668(9)
M(2)−O(6)	2.480(6)	2.443(6)	2.434(7)
M(2)−O(7)	2.720(6)	2.692(6)	2.674(7)
M(2)−O(8)	2.521(6)	2.484(6)	2.468(7)
M(2)−O(9)	2.501(6)	2.459(6)	2.444(7)
M(2)−O(10)	2.558(6)	2.517(5)	2.503(7)
M(2)−O(11)	2.449(7)	2.413(6)	2.392(8)
M(2)−O(12)	2.632(7)	2.596(6)	2.595(8)
M(2)−N(2)	2.676(8)	2.620(7)	2.602(8)
M(2)−N(3)	2.715(8)	2.670(6)	2.654(9)

[a] Symmetry operations used to generate equivalent atoms (#1): $-x+1, -y+1, -z+2$.

One of the interesting features of this structure is the arrangement of the extraframework water molecules (O(100) and O(200)). Two additional molecules of water are generated by center of symmetry. All the water molecules are separated by a distance of ∼2.82 Å and appear to replicate the Z-shape of the tetramers (Figure 3a). Formation of this type of four-membered water cluster is noteworthy, as most of the MOFs contain cyclic water clusters.[27] The O···O distances in regular ice, in liquid water, and in the vapor phase are 2.74, 2.84, and 2.98 Å, and in the present case, the distance between the water molecules indicates that they are similar to liquid H_2O. The stability of the water tetramer has been calculated (B3LYP/6-31+G (d,p)) by means of the Gaussian98 software package.[38] Using the crystal structure geometry, we have made an evaluation of the stability of the water tetramer based on single-point energy calculation

(38) Frisch, M. J.; Trucks, G. W.; Schlegel, H. B.; Scuseria, G. E.; Robb, M. A.; Cheeseman, J. R.; Zakrzewski, V. G.; Montgomery, J. A., Jr.; Stratmann, R. E.; Burant, J. C.; Dapprich, S.; Millam, J. M.; Daniels, A. D.; Kudin, K. N.; Strain, M. C.; Farkas, O.; Tomasi, J.; Barone, V.; Cossi, M.; Cammi, R.; Mennucci, B.; Pomelli, C.; Adamo, C.; Clifford, S.; Ochterski, J.; Petersson, G. A.; Ayala, P. Y.; Cui, Q.; Morokuma, K.; Salvador, P.; Dannenberg, J. J.; Malick, D. K.; Rabuck, A. D.; Raghavachari, K.; Foresman, J. B.; Cioslowski, J.; Ortiz, J. V.; Baboul, A. G.; Stefanov, B. B.; Liu, G.; Liashenko, A.; Piskorz, P.; Komaromi, I.; Gomperts, R.; Martin, R. L.; Fox, D. J.; Keith, T.; Al-Laham, M. A.; Peng, C. Y.; Nanayakkara, A.; Challacombe, M.; Gill, P. M. W.; Johnson, B.; Chen, W.; Wong, M. W.; Andres, J. L.; Gonzalez, C.; Head-Gordon, M.; Replogle, E. S.; Pople, J. A. *Gaussian 98*, revision A11; Gaussian, Inc.: Pittsburgh, PA, 2001.

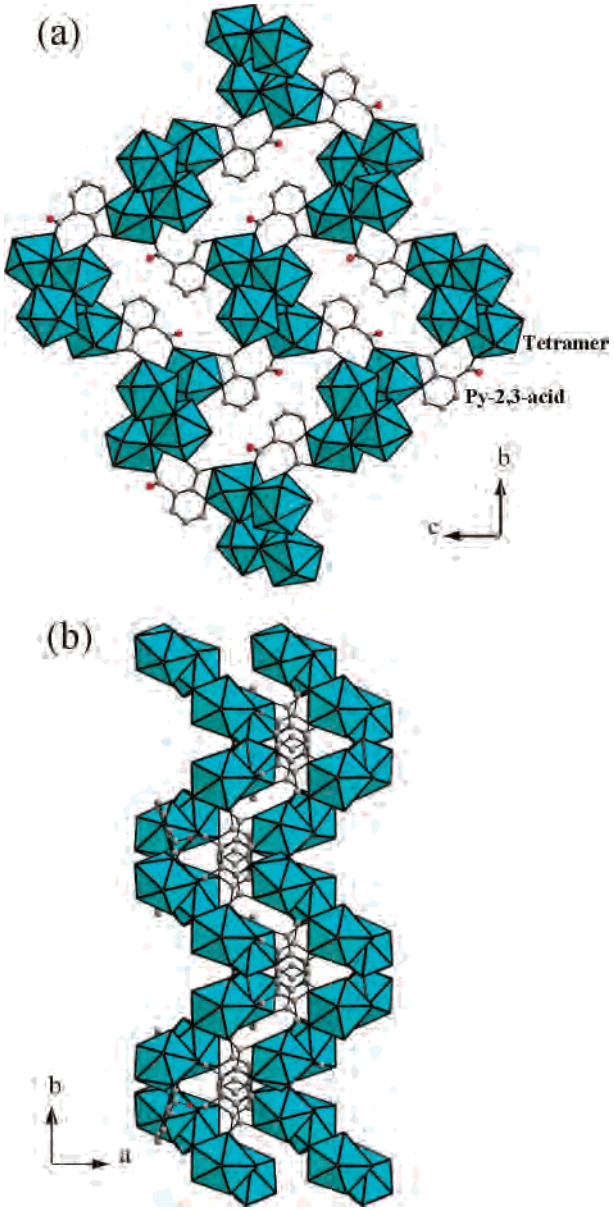

Figure 2. (a) Connectivity between the $M_4O_{24}N_6$, tetramer, and Py-2,3-dicarboxylate (acid-2) forming the two-dimensional layer arrangement. (b) Connectivity between the layers via acid-1 and acid-3. Note that the acid acts like a zipper connecting the two layers.

without the symmetry constraints. The stabilization energy was found to be 19.56 kcal/mol for the water tetramer, which is similar to the conventional hydrogen bond energy in water.[39]

The role of $\pi\cdots\pi$ interactions in the stability of supramolecularly engineered crystal structures has been well documented. In recent years, the role of $\pi\cdots\pi$ interactions in extended structures has been a topic of much interest. In the present compounds, we find significant $\pi\cdots\pi$ interactions between acid-1 and acid-3. The role of $\pi\cdots\pi$ interactions has been discussed in the literature with particular emphasis on the centroid−centroid distances (d) and the angles (θ) suspended between the aromatic rings.[40,41] The centroid−

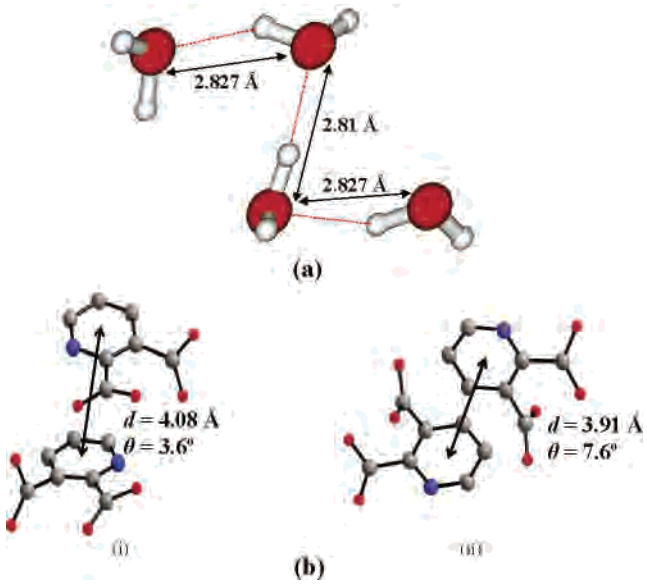

Figure 3. (a) View of the water tetramer. Note the close resemblance to the Ln_4 tetramer. Dotted lines represent possible hydrogen bond interactions between the water molecules. (b) Structure shows the $\pi\cdots\pi$ interactions observed between acid-1 and acid-3 ((i) syn and (ii) trans).

centroid distance (d) and the interplanar angle (θ) between the py-carboxylates are shown in Figure 3b. There are two types of arrangements between the two acids (acid-1 and acid-3), syn and trans, with $d = 4.08$ Å and $\theta = 3.6°$ and $d = 3.91$ and $\theta = 7.6°$, respectively. To understand the nature and the role of the $\pi\cdots\pi$ interactions, we have performed calculations using the AM1 parametrized Hamiltonian available in the Gaussian set of codes.[38] Using the crystal structure geometry, we have made evaluation of the strength of the $\pi\cdots\pi$ interactions. It may be noted that the AM1 method, together with a semiclassical dipolar description, has been employed recently to establish the relationship between the stability and the geometries of organic molecules.[42] In our present case, if we consider a single pyridine-2,3 dicarboxylate, the individual molecules are dipolar and the dipole moment (calculated at AM1 level) is 2.386 D. If we consider the two carboxylates (acid-1 and acid-3) in the syn arrangement (Figure 3b(i)), the net dipole moment is 5.11 D and in the trans arrangement (Figure 3b(ii)), it is 0.734 D. The net $\pi\cdots\pi$ interaction calculations based on the above arrangements of the carboxylates give rise to energies of 4.04 and 4.7 kcal/mol, respectively, for the syn and trans pair. These are typical values, and similar $\pi\cdots\pi$ interaction energies have been observed before.[14]

In Situ Studies. All the three compounds in the present study are isostructural, and for the sake of studying the physical properties, we have chosen the lanthanum containing compound, $[La_2(H_2O)][C_5N_1H_3(COO)_2]_3{\cdot}2H_2O$ (**1**). To understand the nature of the extraframework water molecules, we have carried out in situ XRD studies (Bruker AXS D8 Advance). Variable-temperature in situ powder X-ray diffractions studies were carried out in a 0.7 mm quartz capillary

(39) Scheiner, S. *Hydrogen Bonding: A Theoretical Perspective*; Oxford University Press: Oxford, 1997.
(40) Hunter, C. A.; Sander, J. K. M. *J. Am. Chem. Soc.* **1990**, *112*, 5525.
(41) Hunter, C. A.; Singh, J.; Sanders, J. K. M. *J. Mol. Biol.* **1991**, *218*, 837.
(42) Datta, A.; Pati, S. K. *J. Chem. Phys.* **2003**, *118*, 8420.

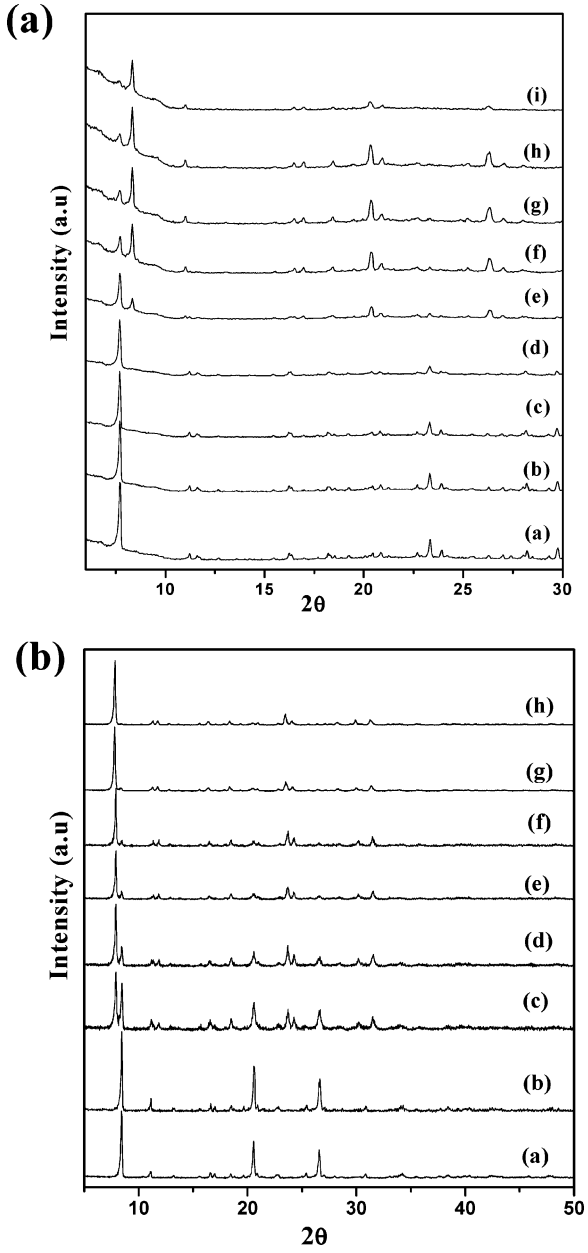

Figure 4. (a) In situ XRD study of $[La_2(H_2O)][C_5N_1H_3(COO)_2]_3{\cdot}2H_2O$. Temperatures of (a) 25, (b) 60, (c) 110, (d) 150, (e) 180, (f) 200, (g) 220, (h) 250, and (i) 300 °C. (b) Ex situ XRD plots of the dehydrated sample of $[La_2(H_2O)][C_5N_1H_3(COO)_2]_3{\cdot}2H_2O$ as a function of time at (a) fully dehydrated, (b) 15, (c) 30, (c) 60, (d) 120, (g) 180, (h) 240, and (i) 300 min.

in transmission geometry with a capillary heater (Huber HTC 9634) from room temperature to 300 °C (Figure 4a). The results indicate that the structure remains unchanged up to 150 °C. The observation of a new peak around $2\theta = 8.3°$, in addition to the main peak at $2\theta = 7.5°$ in the PXRD at 180 °C, indicates a minor change, possibly the contraction of the unit cell. With increasing temperature, the main peak at 7.5° starts to disappear along with an increase in the intensity of the new peak at 8.3°. At 300 °C, the compound appears to be fully dehydrated. To understand the reversibility of the water adsorption, we have carried out ex situ powder X-ray diffraction studies (Philips X'Pert). For this purpose, the sample was dehydrated by heating at 250 °C for 10 h. The dehydrated sample was kept in open air, and

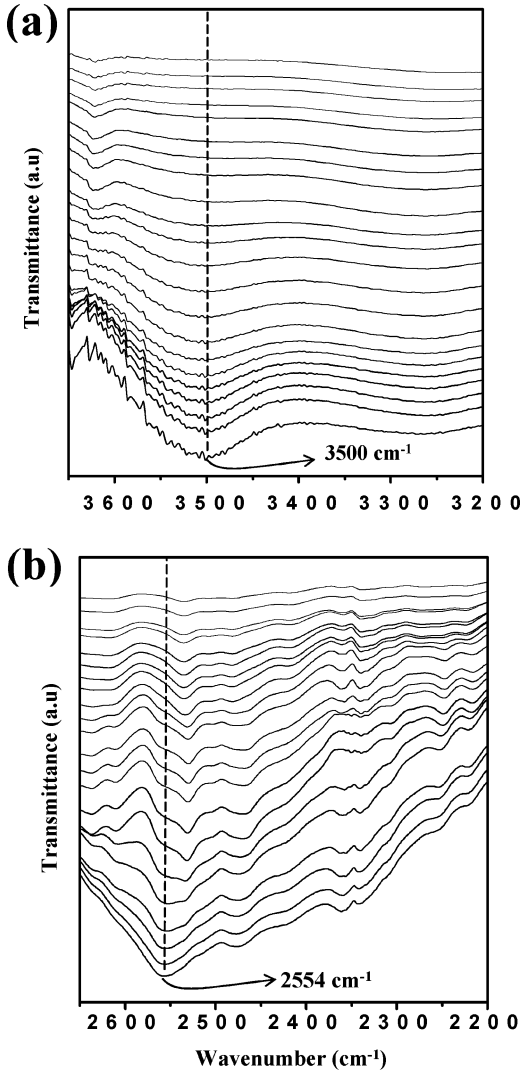

Figure 5. In situ DRIFTS spectra of $[La_2(H_2O)][C_5N_1H_3(COO)_2]_3{\cdot}2H_2O$ as a function of temperature showing the disappearance of the bands at (a) H_2O, 3500 cm^{-1} and (b) D_2O, 2554 cm^{-1}. The dashed line is a guide to the eye.

powder XRD patterns were recorded as a function of time. The results are presented in Figure 4b. As can be seen, the sample starts to rehydrate in about 30 min and the sample appears to be completely rehydrated in ~2 h (Figure 4b)

To understand and prove this reversible hydration behavior of **1**, we have also carried out in situ diffuse reflectance IR spectroscopic (DRIFTS) studies (Perkin-Elmer, SPECTRUM-2000, MCT detector) in the range from room temperature to 270 °C. The extraframework water band at 3500 cm^{-1} was monitored, and the results are presented in Figure 5a. As can be noted, the band at 3500 cm^{-1} gradually disappears with increasing temperature, confirming the removal of the H_2O molecules from the structure. The fully dehydrated sample was exposed to anhydrous D_2O solution for a period of 30 min to rehydrate (deutrate). The IR spectra of this deutrated sample show a peak at around 2554 cm^{-1}, which corresponds to the D_2O stretching vibration.[43] Note that the peak corresponding to water at 3500 cm^{-1} was not observed.

(43) Nakamoto, K. *Infrared and Raman Spectra of Inorganic and Coordination Compounds*; Wiley-Interscience: New York, 1963.

This observation suggests that the extraframework water molecules were completely replaced by D_2O. The temperature-dependent IR spectra studies of the deutrated sample also exhibit a behavior similar to the as-prepared sample when heated under identical conditions. Thus, the peak at 2554 cm^{-1} also loses intensity with increasing temperature (Figure 5b).

The PXRD experiments and DRIFTS FTIR spectroscopy studies clearly indicate that the compound reversibly absorbs the water. Encouraged by the stability of this framework and the reversibility of the hydration−dehydration cycles, we sought to further confirm the microporosity of the La compound by measuring its gas sorption behavior. Attempts to study the gas adsorption behavior using N_2 gas revealed no significant uptake. This may be due to the fact that the kinetic diameter of N_2 (3.64 Å) is larger than that of water (2.64 Å).[44] BET studies on the dehydrated sample using nitrogen as the adsorbate gas give a surface area of 10 m^2/g with a type-II adsorption behavior. The adsorption selectivity can be correlated with the subtle structural transformation during the dehydration of the sample. It is likely that after dehydration, the effective aperture of the one-dimensional channel becomes smaller compared with the kinetic diameter of the adsorbate (N_2). It is important to note that most of the lanthanide coordination frameworks that have been reported are nonporous[45] and demonstrate only solvent sorption.[46,47] This point was brought out by the recent study on Gd imidazoledicarboxylate, which shows open hydrated pores. Upon dehydration, the solid shows only external surface adsorption for O_2, N_2, Ar, and CO_2 but resorbs water,[48] just as in our present study.

Luminescence Studies. It has been shown that the lanthanide-centered emission can be sensitized by molecules having π-systems. Due to the low molar absorptivity of the lanthanides, direct excitation produces only weak emission spectra. Significantly enhanced emission can result when the metals are complexed or chelated with organic moieties that can efficiently absorb and transfer the energy.[3] Generally, direct excitation of the ligand to a singlet state followed by an intersystem crossing (ISC) to a triplet state with the emission from the metal results when a nonradiative energy transfer occurs from the ligand triplet state to the lanthanide ion.[49,50] The newly excited lanthanide ion can then emit a photon or relax via a series of nonradiative processes. This effect is commonly known as the "antenna effect".[51] The pyridine-2,3-dicarboxylate used in the formation of the present compounds absorbs strongly in the UV region and is an attractive ligand for sensitizing the lanthanide ion via the antenna effect. The sodium salt of the pyridine-2,3-dicarboxylate is fluorescent at room temperature and exhibits a broad emission band centered at 370 nm when excited using 300 nm radiation. The emission spectra of the three compounds **1**, **2**, and **3** when excited using 300 nm show a broad emission at ∼370 nm, which indicates that the emission may be due to the intraligand lumiminescence ($\pi^* \rightarrow$ n or $\pi^* \rightarrow \pi$) (Figure 6). The shoulder and low intense peaks in the range from 420 to 530 nm may be due to the other intraligand luminescence of the heterocyclic aromatic system.[52] Recently, the luminescence behavior of Eu-, Tb-, and Yb-doped lanthanide carboxylates was reported by Ferey and co-workers.[53−55] It is believed that the carboxylate ligand acts as the sensitizer for the central lanthanide ion. To investigate the luminescence from the metal center, in the present study we have partially doped Eu (2 mol %, **1a**, and 4 mol %, **1b**) in place of La in **1**. The success of the energy transfer from the pyridine carboxylate to the metal ion is clearly indicated in the suppression of the intraligand emission in the luminescence spectra. A preliminary optical emission of the doped samples **1a** (2 mol % Eu) and **1b** (4 mol % Eu), when observed under UV irradiation, showed pink-red color (Figure 7).

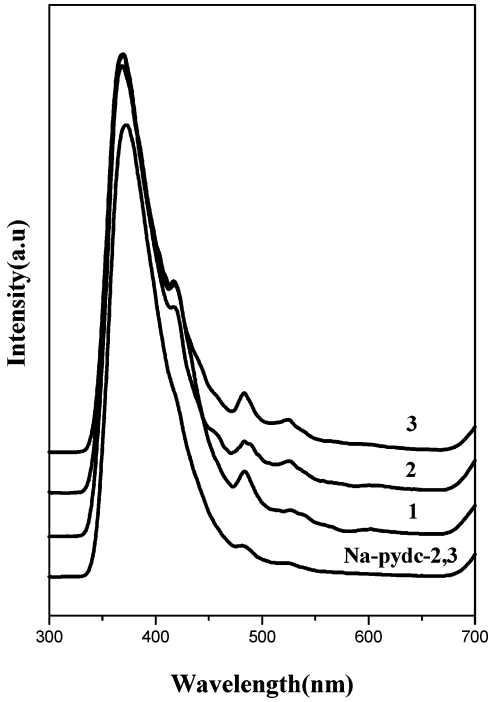

Figure 6. Room-temperature photoluminescence spectra for **1**, **2**, **3**, and the sodium salt of the pyridine-2,3-dicarboxylate.

The room-temperature photoluminescence spectra of the Eu-doped samples are presented in Figure 8. As can be seen, the main intraligand emission band is suppressed followed by the strong red luminescence, characteristic of the $^5D_0 \rightarrow$

(44) Reineke, T. M.; Eddaoudi, M.; Fehr, M.; Kelley, D.; Yaghi, O. M. *J. Am. Chem. Soc.* **1999**, *121*, 1651.
(45) De Lill, D. T.; Gunning, N. S.; Cahill, C. L. *Inorg. Chem.* **2005**, *44*, 258.
(46) Serpaggi, F.; Ferey, G. *J. Mater. Chem.* **1998**, *8*, 2737.
(47) Barbour, L. J. *Chem. Commun.* **2006**, 1163.
(48) Maji, T. K.; Mostafa, G.; Chang, H. C.; Kitagawa, S. *Chem. Commun.* **2005**, 2436.
(49) *Lanthanide Probes in Life, Chemical and Earth Science, Theory and Practice*; Bunzli, J. C. G., Choppin, G. R., Eds.; Elevier: Amsterdam, 1989.
(50) Selvin, P. R. *Nat. Struct. Biol.* **2000**, *7*, 730.
(51) Whan, R. E; Crosby, G. A. *J. Mol. Spectrosc.* **1962**, *8*, 315.
(52) Wen, L.; Li, Y.; Lu, Z.; Lin, J.; Duan, C.; Meng, Q. *Cryst. Growth Des.* **2006**, *6*, 530.
(53) Serre, C.; F. Pelle.; Gardant, N.; Ferey, G. *Chem. Mater.* **2004**, *16*, 1177.
(54) Millange, F.; Serre, C.; Marrot, J.; Gardant, N.; Pelle, F.; Ferey, G. *J. Mater. Chem.* **2004**, *14*, 642.
(55) Serre, C.; Millange, C.; Thouvenot, N.; Gardant, N.; Pelle, F.; Ferey, G. *J. Mater. Chem.* **2004**, *14*, 1530.

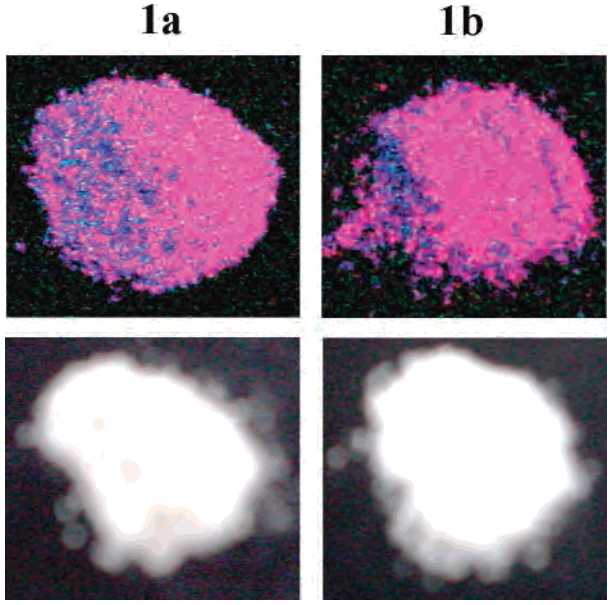

Figure 7. View of the Eu-doped samples 2% Eu (**1a**) and 4% Eu (**1b**) under UV (top) and normal (bottom) illumination.

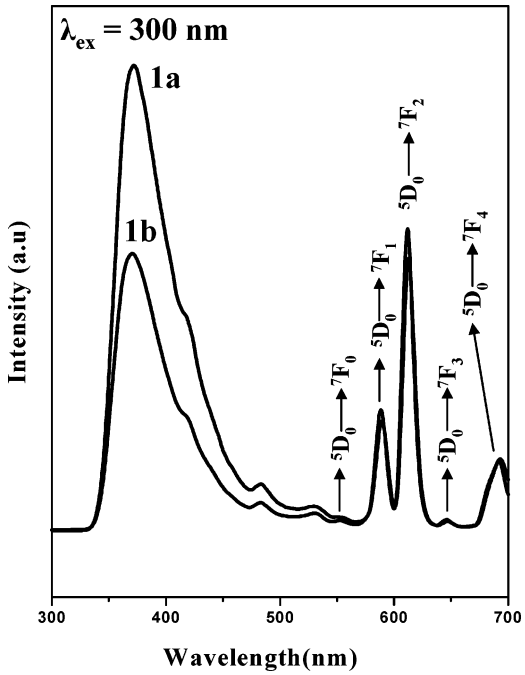

Figure 8. Room-temperature photoluminescence spectra of the doped compounds **1a** and **1b**.

^7F_J ($J = 0, 1, 2, 3, 4$) emission bands of the Eu^{3+} ion.[56] The excitation spectrum of **1a** and **1b** has a band maximum around 300 nm, confirming that the energy transfer takes place from the ligand to the Eu^{3+} ion. Under these circumstances, the ISC from the singlet to triplet excited state of the ligand (pyridine-2,3-dicarboxylate) occurs, followed by the energy transfer to the ^5D_J, $J = 4, 3, 2, 1, 0$, state of the Eu^{3+} ions (Figure 8). The various possible energy levels in the doped compound are given in Scheme 1. The emission from the excited $^5D_0$ level to the ^7F_J ($J = 0, 1, 2, 3, 4$) levels of the Eu^{3+} ion ($4f^6$ configuration) is responsible for the observed red-pink luminescence. Since the $^5D_0$ level will not split by the crystal field (because $J = 0$), the splitting of the emission bands results from the crystal-field splitting of the ^7F_J levels. Thus, the emissions at 558, 588, 612, 646, and 692 nm correspond to $^5D_0 \rightarrow {}^7F_0$, $^5D_0 \rightarrow {}^7F_1$, $^5D_0 \rightarrow {}^7F_2$, $^5D_0 \rightarrow {}^7F_3$, and $^5D_0 \rightarrow {}^7F_4$ transitions, respectively. In the case of **1a** (2 mol % Eu), the overall energy transfer is not complete since the intraligand emission is not fully quenched.[57] For **1b** (4 mol % Eu), on the other hand, the quenching appears to be greater and hence more energy would have been transferred from the ligands to the metal ion (Eu^{3+}). It is likely that the increased concentration of the Eu^{3+} ions in **1b** would have resulted in this behavior. This behavior is not expected to be as linear as it is for higher concentrations of Eu^{3+}; the metal-centered luminescence may be affected by self-quenching. The present results are qualitative in nature, and the emission observed in these compounds could be compared to the emissions observed in other similar compounds.[14] This opens up a new way of introducing luminescent properties into hybrid solids with the extended inorganic−organic structure, where the aromatic linkers (pyridine/benzene dicarboxylate) with delocalized π-electrons acts as an antenna to enhance the optical properties. Further work would be required to fully evaluate and quantify the optical properties of these hybrid compounds.

Scheme 1. Schematic of the Various Levels for the Energy Transfer Process in Ligand-Sensitized Metal-Centered Emissions Observed in the Present Compounds

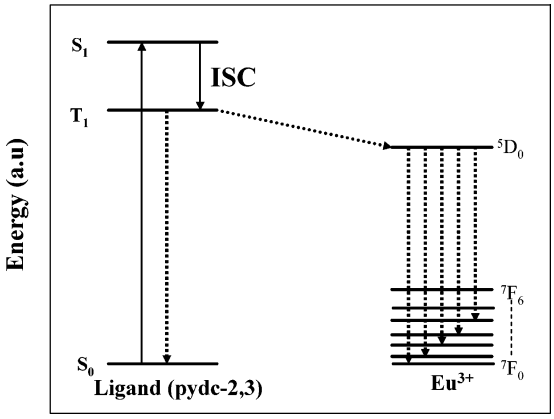

Conclusions

In conclusion, the synthesis, structure, and characterization of a series of isostructural lanthanide coordination polymers have been accomplished. The structures are built up from the expected building units of a coordinated lanthanide ions and carboxylate anions forming the three-dimensional structure. The formation of a novel tetramer, $M_4O_{24}N_6$, is noteworthy. The extraframework water molecules also form a similar four-membered cluster and are fully reversible. The Eu^{3+}-doped samples show red-pink luminescence with characteristic emission corresponding to the $^5D_0 \rightarrow {}^7F_J$ transitions. The emission of the doped samples may be due to the ligand-sensitized energy transfer (or fluorescence resonance energy transfer). We are presently investigating

(56) Sabbatini, N.; Guardigli, M.; Lahn, J. M. *Coord. Chem. Rev.* **1993**, *123*, 201.

(57) Richardson, F. S. *Chem. Rev.* **1982**, *82*, 541.

many other related compounds to understand the luminescence behavior of metal−organic hybrid compounds based on rare-earth elements.

Acknowledgment. We thank Professor S. Vasudevan for the DRIFTS−IR experiments and Dr. Ayan Datta for useful discussion. S.N. thanks the Department of Science and Technology, Government of India, for the award of a research grant. We also thank DST-IRHPA, India, for the CCD facility. S.N. also thanks the Royal Society for a visiting fellowship and the RSC for a travel grant.

Supporting Information Available: X-ray diffraction, thermogravimetric analysis and IR data, bond angles and distances, and CIF data for **1**, **2**, and **3**. This material is available free of charge via the Internet at http://pubs.acs.org.

IC0617644